# Production, $L$ x-ray identification, and decay of the nuclide $^{260}105$†

C. E. Bemis, Jr., P. F. Dittner, R. J. Silva, R. L. Hahn, J. R. Tarrant, L. D. Hunt, and D. C. Hensley
*Oak Ridge National Laboratory, Oak Ridge, Tennessee 37830*
(Received 9 May 1977)

The nuclide $^{260}105$ has been produced in the $^{249}Cf(^{15}N,4n)$ reaction and its decay properties investigated. The $\alpha$-decay branch of $1.52 \pm 0.13$-sec $^{260}105$ has been measured to be $(90.4 \pm 0.6)\%$ with spontaneous-fission decay the remainder $[(9.6 \pm 0.6)\%]$. Measured $\alpha$-particle energies and intensities (% per decay) are $9.041 \pm 0.014$ MeV $(48 \pm 5)$, $9.074 \pm 0.014$ MeV $(25 \pm 3)$, and $9.120 \pm 0.017$ MeV $(17 \pm 3)$. Characteristic $L$-series x rays of element 103 were observed in coincidence with these $\alpha$-particle groups, thus providing elemental identification. The $^{256}Lr$ $\alpha$-decay daughter was observed in a direct time-correlated genetic linkage, thus providing the mass number assignment. The absence of characteristic $L$- or $K$-series x rays of element 104 in time coincidence with, but preceding, spontaneous-fission-decay events, has allowed an upper limit of 2.5% to be placed on the electron-capture decay branch of $^{260}105$ to the elusive nuclide 0.1-sec $^{260}104$. If $^{260}104$ is a spontaneous-fission emitter with a half-life $\leq 100$ $\mu$sec, as some predictions would indicate, then the electron-capture decay branch of $^{260}105$ is $\leq 0.2\%$.

[RADIOACTIVITY $^{260}105$ [from $^{249}Cf(^{15}N,4n)$ reaction]; measured $t_{1/2}$, $E_\alpha$, $I_\alpha$, $E_{SF}$, $I_{SF}$, $I_{EC}$, $E_X$, $L_X$, $E_\gamma$, $I_\gamma$; $\alpha$-$X$ coin. and SF-$X$ coin. $\alpha$-$\alpha$ time correlation; deduced $^{256}Lr$ levels, $J$, $K$, $\pi$ $\alpha$ hindrance, SF hindrance, atomic number mass number. Enriched target.]

## I. INTRODUCTION

The characterization of isotopes of the heaviest elements is often extremely difficult, as these nuclides can only be produced in heavy-ion induced nuclear reactions at rates which rarely exceed a few atoms per hour. It is not surprising, therefore, that experiments dealing with these short-lived nuclides are often somewhat less than definitive and that discovery claims for new elements, particularly those for elements 104 and 105, have been surrounded by controversy and counterclaims by rival experimental groups (see, e.g., Ref. 1). Earlier work done at this laboratory[2,3] has demonstrated that the coincident observation characteristic x rays emitted following the $\alpha$ decay can provide definitive elemental identifications of the transfermium nuclides even though only a few hundred atoms were available for study. Nuclear spectroscopic and structure information can also be obtained in the transfermium region of the nuclear Periodic Table by the coincident observation of the decay $\gamma$ rays.[4-6] Although the observations of characteristic x rays following $\alpha$ decay probably provides the most definitive elemental identifications, another technique, particularly well suited for studies of the heaviest elements, is the genetic-linkage method. In this latter case, a genetic link is established between the $\alpha$ decay of a parent nuclide and the subsequent decay of the previously well-characterized daughter nuclide by the observation of the time-correlated parent and daughter decay events. The genetic-linkage method has been used to great advantage to provide identifications for the short-lived $\alpha$-emitting isotopes of elements 104–106.[7-10]

The first claim for the production of an isotope of element 105 was made in 1967 by Flerov,[11] and a more complete description of this work appeared in 1968.[12] A 9.7-MeV $\alpha$ activity produced in the bombardment of $^{243}Am$ with $^{22}Ne$ ions was said to arise in the decay of $^{260}105$, or possibly $^{261}105$, from the observation of fewer than 10 time-correlated pairs of $\alpha$ events linking this activity to an element 103 daughter activity. A 9.4-MeV $\alpha$ activity, also produced in these experiments, was associated with the decay of $^{261}105$. An ~2-sec spontaneous-fission activity was subsequently observed[13-15] in reaction of $^{243}Am$ with $^{22}Ne$ ions and ascribed to the decay of either $^{260}105$ or $^{261}105$; nuclidic agreement from such experiments with spontaneous-fission activities is often ambiguous because of the nonspecificity of this decay process. Comparative gas-phase chemical studies using this spontaneous-fission activity were subsequently performed by Zvara *et al.*[16] and were claimed to support the 105 elemental assignments although the mass assignment, either $^{261}105$ or $^{260}105$, remains ambiguous.

Ghiorso and coworkers[8] produced $^{260}105$, a 1.6-sec $\alpha$ activity, in 1970 using the $^{249}Cf(^{15}N,4n)$ reaction. $\alpha$-particle groups of 9.06, 9.10, and 9.14 MeV were attributed to the decay of $^{260}105$ and the assignment was based on the establishment of a genetic link to the previously known ~30-sec $^{256}Lr$ $\alpha$-decay daughter nuclide. These workers[8] also

reported that they were not able to produce the 9.4- and 9.7-MeV $\alpha$ activities and hence confirm the earlier experiments of Flerov *et al.*,[11,12] and they therefore claimed discovery of element 105. The name hahnium was proposed for this new element.[8] Druin *et al.*[17] subsequently repeated the earlier $\alpha$-decay experiment of Refs. 11 and 12 ($^{243}$Am + $^{22}$Ne) with an improved technique and reported a $(1.4^{+0.6}_{-0.3})$-sec $\alpha$ activity, with energies of 8.9 and 9.1 in addition to 9.4 MeV, which was linked genetically to a 35-sec daughter activity with $\alpha$ energies in the range 8.3–8.6 MeV. The daughter nuclide was presumed to be either $^{256}$Lr or $^{257}$Lr, but subsequently, $^{256}$Lr was shown[41,42] to have a half-life of 25.9 sec with $\alpha$-particle energies in the range 8.30–8.65 MeV and $^{257}$Lr, a half-life of 0.6 sec with $\alpha$-particle energies of 8.80 and 8.86 MeV. Thus, all of the $\alpha$ activities of Ref. 12 and Ref. 17, the 8.9-, 9.1-, and 9.4-MeV activities, must be assumed to be linked to the decay of $^{260}$105 and not to the decay of $^{261}$105.

Refinements in the spontaneous-fission experiments ($^{243}$Am + $^{22}$Ne) have also been made by Flerov *et al.*, [18] and a more accurate half-life value of $1.8 \pm 0.6$ sec reported, although the mass assignment favored by these workers is $A = 261$. Flerov *et al.*[18] have proposed the name nilsbohrium for element 105, claiming discovery, as they have repeated and confirmed their earlier[13] spontaneous-fission experiments.

These element 105 discovery claims are contested and have yet to be resolved. Further experiments by Ghiorso *et al.*[9] have since produced two new $\alpha$ activities, $^{261}$105 ($t_{1/2} = 1.8 \pm 0.6$ sec, $E_\alpha = 8.93$ MeV) and $^{262}$105 ($t_{1/2} = 40 \pm 10$ sec, $E_\alpha = 8.45$–$8.66$ MeV). The assignments are based on genetic links to 0.6-sec $^{257}$Lr and 4.5-sec $^{258}$Lr, respectively. The comparative-chemical studies have since been reinvestigated by Zvara *et al.*[19] with essentially the same conclusions as in earlier experiments,[16] namely, that the ~2-sec spontaneous-fission activity produced in the $^{243}$Am($^{22}$Ne, $5n$)$^{261}$105 reaction agrees in its chemical behavior with that expected for element 105 (ekatantalum).

In this present work, we have applied both the definitive coincident characteristic x-ray and the direct genetic-linkage identification techniques to a study of the decay of $^{260}$105. A thorough investigation of the decay properties of this nuclide performed using methods substantially different but complementing those used previously by other workers was deemed essential if our experiments would be of value in addressing the conflicting discovery and identification claims. The observation of element 103 characteristic x rays following, and in coincidence with, the $\alpha$ decay would provide elemental identification. Direct genetic-linkage experiments, where the $\alpha$ particles of both the 105 parent and 103 daughter activities are observed in time correlation, should provide mass identification if the daughter activity has been previously identified and characterized. Obtaining experimental data on half lives, production yields, and other decay modes, and the establishment of accurate energies, were also objectives of our experimental work

Of particular interest to us was the possibility of linking directly and definitively, for the first time, the atomic number of $^{260}$104 to its decay properties. Should the nuclide $^{260}$105 have an appreciable decay branch via electron capture,[8] in addition to the expected dominant $\alpha$-decay branch, electron-capture decay would lead to the nuclide $^{260}$104. The nuclide $^{260}$104, reported to be a short-lived even-even spontaneous-fission activity, is the subject of the hotly contested element 104 discovery controversy[1,18,20-30] similar to that described for element 105 above. Characteristic x rays would be emitted in the atomic rearrangements following electron capture, in this case characteristic of element 104, and the observation of these x rays preceding, but in delayed coincidence with, spontaneous-fission decay would be the basis of an unequivocal identification of this elusive isotope of element 104. This electron-capture method may be the only technique capable of providing a definitive identification for short-lived even-even spontaneous-fission activities in the transfermium element region, although it is possible that a measurement of the total kinetic-energy release in fission[31] would also provide some selectivity for spontaneous-fission activities in this mass region. These experimental results together with our conclusions are given in this present work.

## II. EXPERIMENTAL PROCEDURE

### A. Production of $^{260}$105

The $^{249}$Cf($^{15}$N, $4n$) reaction was used to produce the atoms of $^{260}$105 for these experiments. Ghiorso *et al.*[8] have experimentally estimated the production cross section for this reaction to be ~3 mb at a $^{15}$V ion energy of ~85 MeV, which is in good agreement with our calculated[32-34] peak cross section of 4.5 nb at 86.0 MeV. A $^{249}$Cf target 635 $\mu$g/cm$^2$ was prepared by electrodeposition of the nitrate from an isopropyl alcohol medium onto a 2.35 mg/cm$^2$ Be (12.7 $\mu$m) backing foil using isotopically pure $^{249}$Cf which had previously been recovered as the decay product of initially pure $^{249}$Bk. The deposit covered an area of 0.37 cm$^2$ and the californium was converted to the oxide ($Cf_2O_3$) by heating in air.

The heavy-ion bombardments were performed

at the Oak Ridge Isochronous Cyclotron (ORIC) using $^{15}N^{+4}$ ions accelerated to an energy of 99.1 MeV and using $N_2$ gas isotopically enriched to ~99% in $^{15}N_2$ as the cyclotron ion source feed gas. After extraction from the cyclotron and transport to the experimental station, the ion beam passed through a 2.35 mg/cm$^2$ Be (12.7 $\mu$m) isolation window separating a small helium filled reaction chamber from the cyclotron vacuum system. After traversing the Be entrance window and the Be foil target backing, the incident $^{15}$Ne beam had been reduced in energy to ~86.0 MeV, an energy which corresponds to the expected peak cross section for the $^{249}$Cf($^{15}$N, 4$n$) reaction. The reaction chamber was filled with unadulterated helium gas to a pressure of 860 Torr to thermalize the reaction products recoiling from the $^{249}$Cf target due to large linear momentum transfer from the incident beam. The recoil range for the most energetic $^{260}$105 reaction products is ~500 $\mu$g/cm$^2$ in $Cf_2O_3$ and thus only ~70% of the target material could contribute recoils which could be thermalized in the helium gas. The helium gas and the entrained reaction products were continually pumped from the reaction cell through a 0.343-mm diam nozzle using a high speed vapor-booster type diffusion pump. The reaction products emerging from the helium jet impinged and were collected on an aluminized plastic tape. Under the conditions of this experiment, the helium flow rate through the ~4 cm$^3$ recoil thermalization chamber was 45 Torr liter sec$^{-1}$. With a pumping speed of 2000 liter sec$^{-1}$, the vapor booster pump could easily maintain a pressure of $2\times 10^{-2}$ Torr in the separate vacuum system containing the collector tape. The overall collection efficiency for the system is estimated to be ~80% based on our previous studies using heavy-ion reactions with known production cross sections.

The $^{15}$N beam exited from the reaction cell through two additional windows of 2.35 mg/cm$^2$Be, the first of which defined the active volume of the recoil thermalization region. The $^{15}$N beam was finally dumped downstream in a water-cooled Faraday cup used in measurements of the beam current. The helium-filled reaction-cell assembly was water cooled and chilled helium gas was circulated between the front Be entrance foil and the target backing foil as well as between the two Be exit foils. Beam current levels were kept below ~4.5 $\mu$A, measured as the fully stripped ion ($^{15}N^{+7}$), in order to avoid localized overheating effects in the Be entrance and exit foils.

### B. Tape transport assembly and detection system

A fast tape-transport system was designed and developed to move periodically a spot of activity collected on aluminized plastic tape from the gas-jet recoil chamber to a detection and measurement station located above the heavy concrete shielding of the cyclotron bombardment station. The use of a tape system, to move collected radioactivities to a low-background environment where high-resolution spectroscopic studies may be performed, was considered more advantageous than the use of a long capillary tube connected directly to the gas-jet assembly. Capillary tube systems are often characterized by poor or indeterminate transport efficiency ($\lesssim$ 50%), and usually require an adulterant in the He gas, such as NaCl vapor, $CCl_4$, or benzene. These adulterants can interfere with subsequent $\alpha$-particle energy measurements and/or be decomposed in the vicinity of the target by the intense heavy-ion beam. These difficulties were obviated in these experiments by the use of the tape-transport assembly outlined in Fig. 1.

A continuous belt of aluminized plastic tape, ~7.5 m long × 2.54 cm wide × 0.010 cm thick, was driven by two identical drive assemblies, each consisting of a 1-hp 3600-rpm motor, an electromagnetic clutch and brake, a high-vacuum rotary feedthrough, and a rubber-coated magnesium drive wheel, 26 cm in diameter. Both tape-drive assemblies, one located in the bombardment room and the other located in a low-background counting room directly above, were driven simultaneously using programmable digital logic modules. A photodiode and lamp assembly, used to detect holes perforated in one edge of the tape at 2.54-mm intervals, served as the digital feedback indicator in positioning the tape. The drive wheels, photodiode and lamp assembly, and the silicon surface-barrier detectors used to detect $\alpha$ particles and fission fragments, were enclosed in a vacuum system common to the gas-jet outlet. The tape was constricted by guides and rollers to pass thru a ~5-cm-i.d. pipe connecting the bombardment station assembly with the assembly containing the detectors in the counting area located directly above.

The tape-drive system was programmed to move the spot of activity collected at the gas-jet orifice a distance of ~3.4 m and position it in front of the first of two specially constructed 2-cm$^2$ silicon (Au) surface-barrier detectors. This surface-barrier detector viewed the spot of collected activity directly after transport; the second detector was a background detector, used to assess the buildup on the tape of long-lived activities which could interfere with the measurements of $^{260}$105. Each detector subtended a solid angle of ~35% of 4$\pi$ sr from the tape for a spot of activity on the detector axis. The detectors, of a special close-mounting design, had an entrance window of ~20 $\mu$g cm$^{-2}$ of Au instead of the usual 40 $\mu$g cm$^{-2}$ to reduce the

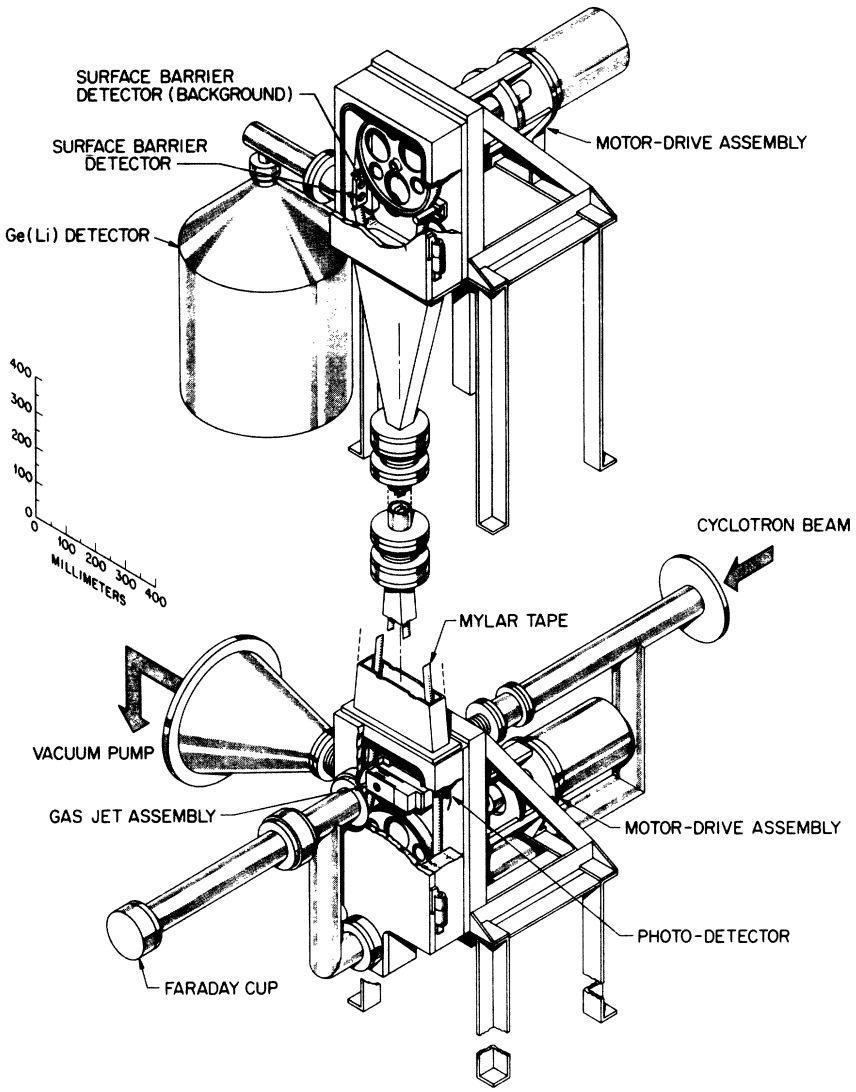


FIG. 1. Cutaway view of the tape-transport system and gas-jet assembly used to transfer reaction product recoil atoms to the detection station.

$\alpha$ peak broadening due to energy-loss-straggling effects arising in our high detection geometry application. An intrinsic- planar-Ge photon detector, 10 cm$^2$ in area and 1.2 cm thick with a 0.25-mm Be entrance window, viewed the spot of collected activity in opposition to the first surface-barrier detector. A 0.51-mm thick Be window mounted in the wall of the vacuum system next to the tape and opposite the surface-barrier detector permitted the Ge detector to be placed in close proximity to the spot of collected activity. Under the conditions of our experiments, the absolute photopeak detection efficiency for photons in the energy range 10–40 keV was ~30%; and for photons in the range 115–130 keV, ~20%.

A spot of activity collected at the gas-jet orifice could be transported and positioned in front of the first surface-barrier detector within 180 msec. The tape system was programmed to advance at 3-sec intervals, approximately two half-life periods for $^{260}$105, thus positioning a new spot of collected activity in front of the first detector. In order to establish a direct time-correlated genetic link between the decay of $^{260}$105 and its $\alpha$-decay daughter $^{256}$Lr, the tape-system drive was programmed to stop for a period of 35 sec whenever an $\alpha$ event in the range $9.0 \leq E_\alpha$ (MeV) $\leq 9.2$ was detected in the first surface-barrier detector. $\alpha$ events in the decay of $^{260}$105 were expected in this energy range, and the additional 35-sec counting period was sufficiently long to allow observation of most of the subsequent $^{256}$Lr $\alpha$ decay.

$\alpha$ events occurring in this "extended" mode of operation were digitally tagged for special data processing.

### C. Data Acquisition methods and processing

$\alpha$- and spontaneous-fission-event pulses occurring in the two surface-barrier detectors were processed through two linear amplification chains each in order to cover pulse height ranges suitable for both $\alpha$ spectroscopy [$E_\alpha$ (MeV) $\lesssim$ 12.00] and for singles fission-fragment spectroscopy [$E_{FF}$ (MeV) $\lesssim$200]. Pulses with an energy $\gtrsim$5 MeV occurring in the first surface-barrier detector were also used to start a time-to-pulse-height converter (TPHA) with a time range of 80 $\mu$sec. Photon pulses in the energy range $10 \lesssim E$ (keV) $\lesssim$300 occurring in time coincidence with these $\alpha$ events, and during the duration of the TPHA, were then processed with the corresponding $\alpha$ pulse and with the TPHA pulse. All $\alpha$ and fission events occurring in the two detectors were processed whether or not photon events were detected in coincidence with events in the main surface-barrier detector. Amplified pulses from the detectors were gated into linear analog pulse stretchers and sequentially digitized using a single multiplexed 8192 channel analog-to-digital converter system as described by Goodman[35] and by Hensley.[36] Each list-mode data word characterizing a decay event contained the digitized $\alpha$-particle and fission-fragment pulse heights from the two surface-barrier detectors, the digitized photon, and the TPHA pulse heights, and the contents of digital scalers which indicated other experimental conditions such as the time in msec of the occurrence of the event relative to the start of a counting cycle, the cycle sequence number, and the digitized integral beam current. The list-mode data words were buffered onto, and temporarily stored in, disc memory and later transferred to magnetic tape for permanent storage and subsequent off-line analysis.

An additional mode of operation of the data acquisition system was also used in these experiments so that characteristic $L$- or $K$-series x rays of the transfermium elements ($100 \lesssim Z \lesssim 105$) preceding spontaneous-fission events could be observed in a delayed time correlation. This type of decay event could arise in the electron capture or in the isomeric internal-conversion decay of a parent activity which is then followed by spontaneous fission of the daughter activity, i.e., in the $^{260}105$ (EC) $\rightarrow$ $^{260}104$ (SF) sequence. Photon events occurring in the energy ranges 10–35 keV ($L$-series x rays) and 110–165 keV ($K$-series x rays) were gated into a special pulse stretcher and held for a maximum of 100 $\mu$sec before processing to await the subsequent occurrence of any fission event. If these special photon events were followed within the 100 $\mu$sec delay period by an $\alpha$ or fission event, the event data word automatically included the digitized pulse height of this "prior" x ray. When these pulses were not followed by fission or $\alpha$ events within the 100 $\mu$sec delay period, they were processed separately with the contents of two digital scalers, one of which indicated the time in $\mu$sec from the end of bombardment, and the other the cycle sequence number. These "prior" x ray single events were thus truncated in order to reduce the number of magnetic tapes required for data storage. This special feature of the acquisition system hardware and software, the "prior" x-ray" mode, was tested and developed using 2.6-sec $^{214}$Ra, produced in $^{12}$C ion bombardments of Pb, which decays to 5.4 msec $^{214}$Fr via a 0.06% electron-capture decay branch. The $\alpha$ decay of $^{214}$Fr was observed in time correlation with preceding x rays characteristic of Fr ($Z$ = 87).

The $\alpha$-particle-energy and -efficiency calibrations for both surface-barrier detectors were established using sources of $^{244}$Cm, $^{241}$Am, $^{243}$Am, and $^{249}$Cf, and the calibrations were extended to higher energies using a precision pulse generator. The $\alpha$-particle energies are referred to $E\alpha_0(^{244}\text{Cm}) = 5.8049$ MeV, $E\alpha_{75}(^{243}\text{Am}) = 5.2748$ MeV, and $E\alpha_{383}(^{249}\text{Cf}) = 5.8135$ MeV as suggested in the $\alpha$-energy and intensity evaluation of Rytz.[37] The energy and efficiency calibrations for the photon detector were also established with these same standard sources; the absolute photopeak detection efficiencies as a function of photon energy were obtained from "singles" spectra and from spectra obtained in coincidence with $\alpha$ particles observed in the main detector. Corrections for true coincidence summing effects in the photon detector, particularly for the various $L$- and $K$- series x rays, were often required to obtain the absolute efficiencies in some cases because of the high geometry and thus high efficiency of the photon detector. Photon energies are referred to the energies of the most prominent $L$-series x rays ($L\alpha_1$, $L\beta_2$, $L\beta_1$, $L\gamma_1$, etc.) and $K$-series x rays ($K\alpha_2$, $K\alpha_1$, $K\beta_1$, $K\beta_2$) in Np, Pu, and Cm as derived from a forthcoming summary and evaluation of Porter and Freedman.[38] The $L$-series x-ray intensities reported in Ref. 39 and the energies and intensities of prominent $\gamma$-ray and $K$ x-ray lines reported in Ref. 40 were also used.

A nominal $\alpha$-particle-energy resolution of ~35 keV was maintained during the course of these experiments, primarily limited by differential energy-loss and straggling effects in the Au window in this high geometry application. The measured photon energy resolution was ~600 eV for $\gamma$ rays with

energies in the range 100–120 keV and ~300 eV for photons in the energy range 10–40 keV.

After these experiments were completed, the magnetic tapes containing the raw experimental list-mode data were scanned to yield information on the decay of nuclides produced in $^{15}$N ion reactions on $^{249}$Cf. Multiple scans of the ~50 data tapes were required in order to explore fully the various correlations between the data parameters recorded in these experiments.

## III. RESULTS AND DISCUSSION

Over 200 000 bombardment-counting cycles were completed during the course of these experiments and the total integrated $^{15}$N beam that passed thru the target assembly was 1.87 C. Our results are given below.

### A. $\alpha$ spectral analysis

The $\alpha$-particle-energy spectrum for nuclides produced in 86.0-MeV $^{15}$N ion bombardments of $^{249}$Cf and for the time interval 0.18–3.18 sec after bombardment is shown in Fig. 2. The $\alpha$-particle assignments to particular nuclides, as indicated in Fig. 2, are based on the correspondence in energy and half-life with those of previously known and well established $\alpha$ emitters. For most of the assignments in Fig. 2, the identifications were confirmed by the observation of characteristic $L$-series and/or $K$-series x rays of the daughter elements in coincidence with the particular $\alpha$ group. A continuum-type background underlying most $\alpha$ peaks, particularly those below ~8.0 MeV, is readily apparent by an inspection of Fig. 2. This continuum-type background decayed with a half-life of 817 ± 14 msec and is associated with the $\beta^-$ decay of $^{8}$Li to $^{8}$Be, which is unstable to decay into two $\alpha$ particles. The nuclide $^{8}$Li can readily be produced in direct reactions of $^{15}$N with the Be target backing. $\alpha$ groups arising in the decay of nuclides produced in the reactions of $^{15}$N ions with minute Pb and Bi impurities in the $^{249}$Cf target material and/or in the Be target backing were also observed in these experiments. Although most of the nuclides produced from the Pb and Bi impurities are very short lived and would not have been detected in these experiments because of the finite gas-jet and tape-transport times, some of the longer-lived nuclides could be identified in these experiments, such as $^{212}$At (0.30 sec), $^{213}$Fr (34.7 sec), and $^{215}$Ac (0.17 sec).

The $\alpha$-particle events with energies in the range 9.0–9.2 MeV were assigned to the decay of $^{260}$105. Three distinct $\alpha$ groups with energies in MeV (and relative intensities) of 9.041 ± 0.04 (1.00), 9.074 ± 0.014 (0.52 ± 0.08), and 9.120 ± 0.017 (0.35 ± 0.04) were unfolded from this portion of the $\alpha$ spectrum by an iterative curve-fitting procedure using a semi-Gaussian function characteristic of the re-

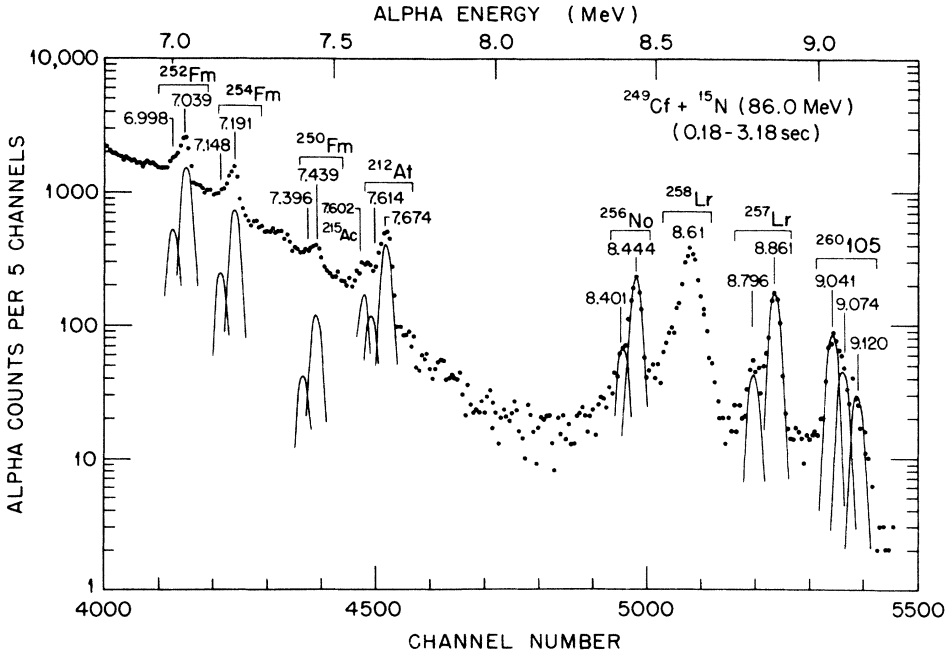


FIG. 2. $\alpha$-particle-energy spectrum from radioactivities produced in reactions of 86.0-MeV $^{15}$N ions with $^{249}$Cf in the time interval 0.18–3.18 sec following bombardment.

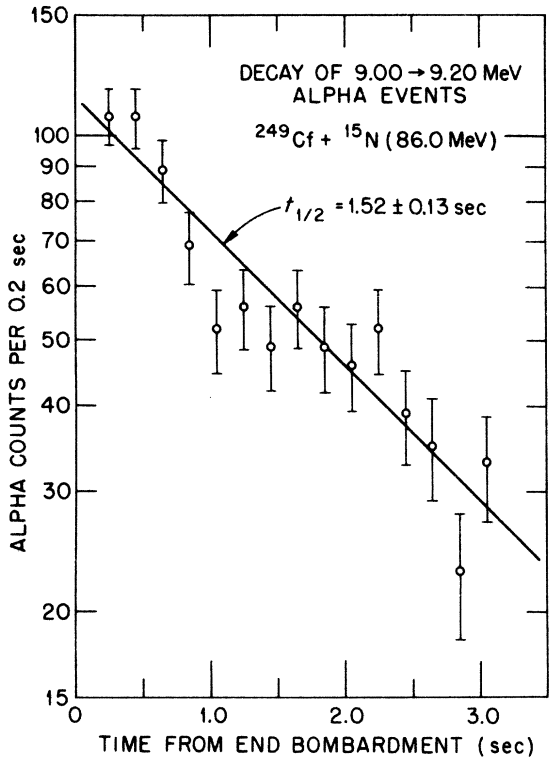


FIG. 3. Time distribution of $\alpha$-particle events in the energy range 9.00–9.20 MeV following bombardment of $^{249}$Cf with 86.0-MeV $^{15}$N ions.

sponse of the detector to monoenergetic $\alpha$ particles of the above energies. Each of the three $\alpha$ groups decayed with the same half-life and the composite decay of all $\alpha$ particles with energies in the range 9.00–9.20 MeV, a total of 871 events, is shown in Fig. 3. A half-life of 1.52 ± 0.13 sec was derived using a one-component exponential least-squares fitting procedure. The energies and relative intensities of these $\alpha$ groups and the half-life for $^{260}$105 are in excellent agreement with those previously reported for $^{260}$105 by Ghiorso *et al.*[8]

The $\alpha$-decay daughter nuclide of $^{260}$105, (25.9 ± ± 1.7)-sec $^{256}$Lr, is obscured in the $\alpha$ spectrum displayed in Fig. 2 by the relatively intense $\alpha$ groups at 8.401 and 8.444 MeV arising in the decay of (3.04 ± 0.14)-sec $^{256}$No. The $\alpha$ spectrum of $^{256}$Lr is quite complex[41,42] with $\alpha$ groups in the range 8.3–8.7 MeV, the most intense of which is the (8.430 ± 0.015)-MeV group which occurs in (38.3 ± 2.9)% of the $\alpha$ decays of $^{256}$Lr. As described in Sec. II C, the normal 3-sec tape-cycle period was automatically extended for an additional 35 sec whenever an $\alpha$ event in the range 9.0–9.2 MeV., i.e., those expected from $^{260}$105, was detected. When such parent $\alpha$ events do occur, the $\alpha$-decay daughter atom recoils and remains embedded in the tape and, if the observation period is sufficiently long, subsequent $\alpha$ events in the decay of the daughter nucleus may also be observed and directly correlated with the parent $\alpha$ events. The $\alpha$-particle-energy spectrum in the energy range 8.0–8.8 MeV accumulated during all such 35-sec extended tape-cycle periods is shown in Fig. 4, and the complex $\alpha$-group structure of $^{256}$Lr is readily discernible. From the number of $\alpha$ events observed and ascribed to the decay of the $^{260}$105 parent, 871 events in Fig. 2, the number of $\alpha$ events expected to be observed from an $\alpha$-decay daughter nuclide with a (25.9 ± 1.7)-sec half-life in a

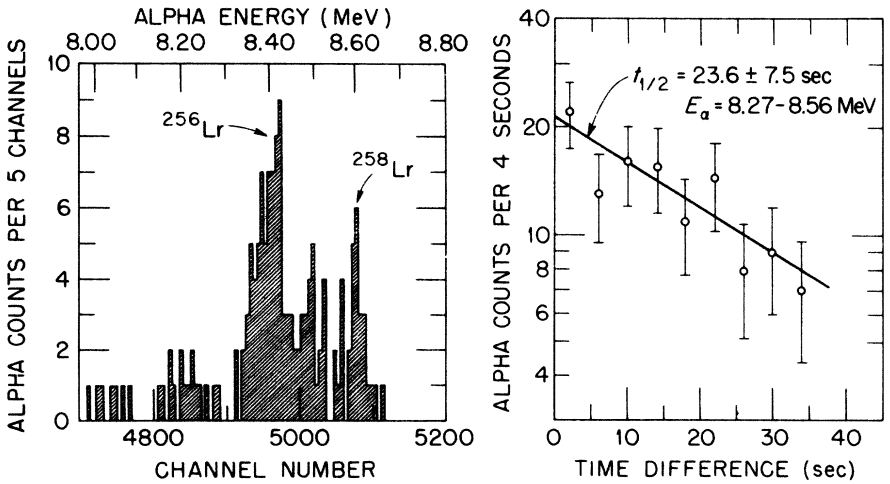


FIG. 4. $\alpha$-particle-energy spectrum (left portion) for activities directly correlated with a preceding $\alpha$ decay in the energy range 9.00–9.20 MeV. The time distribution of these events in the energy 8.27–8.56 MeV is shown in the right-hand portion.

subsequent 35-sec interval, under the conditions of our experiment, is $122 \pm 11$. In the spectrum displayed in Fig. 4, 113 events may be ascribed to the decay of $^{256}$Lr, in excellent agreement with the expected value. The decay of the $\alpha$ events in the energy interval 8.27–8.56 MeV, relative to the time of occurrence of the parent $\alpha$ event, is also displayed in Fig. 4 and we have derived a half-life value of $23.6 \pm 7.5$ sec for these events using a one-component least-squares fitting procedure. This derived half-life is in agreement with the $(25.9 \pm 1.7)$-sec value expected for $^{256}$Lr. Based on estimated[32–34] and measured[41,42] relative production cross sections for $^{249}$Cf($^{15}$N; $\alpha$, $2n$)$^{258}$Lr, $^{249}$Cf($^{15}$N; $\alpha$, $3n$)$^{257}$Lr, and $^{249}$Cf($^{15}$N; $\alpha 4n$)$^{256}$Lr of 1.0 : 0.92 : 0.018, respectively, fewer than 10 $\alpha$ events due to directly produced $^{256}$Lr are expected in the $\alpha$ particle singles spectrum in Fig. 2, and ~0.4 events due to directly produced $^{256}$Lr are expected in the correlated spectrum in Fig. 4. Supporting this conclusion is the result that the entire $\alpha$-group structure at ~8.4 MeV in Fig. 2 may be solely accounted for by 3.04-sec $^{256}$No based on our observed yield of coincident $L$ x rays of Fm. Each of the three $\alpha$ groups ascribed to the decay of $^{260}$105, the 9.041-, 9.074-, and 9.120-MeV groups, produced time-correlated $\alpha$ events of $^{256}$Lr confirming our energy and intensity results for $^{260}$105 from analyses of the $\alpha$ spectrum of Fig. 2.

The 24 $\alpha$ events ascribed to 4.35-sec $^{258}$Lr in Fig. 4 arise from chance or random correlations and are the correct number of such events $(23 \pm 4)$ expected based on a $(4.35 \pm 0.59)$-sec half-life and the 3285 $\alpha$ events ascribed to $^{258}$Lr in the spectrum of Fig. 2. No evidence for $(0.646 \pm 0.025)$-sec $^{257}$Lr with $\alpha$ events in the range 8.7–8.9 MeV was found, nor was any expected, in the time correlated 35-sec $\alpha$ spectrum, although the decay of this nuclide was readily apparent in the primary spectrum shown in Fig. 2.

We conclude from our analysis of the $\alpha$ spectrum and from the time and number correlations associated with the daughter nuclide $^{256}$Lr that $^{260}$105 is a $(1.52 \pm 0.13)$-sec $\alpha$ activity with three $\alpha$ groups in the range 9.00–9.15 MeV.

### B. Spontaneous-fission decay

All events detected in the surface-barrier detectors with an energy greater than ~15 MeV were processed also in parallel lower-gain amplifiers suitable for fission-fragment spectroscopy. Single-fragment spontaneous-fission events ($40 \leq E_{ff}$ (MeV) $\leq 140$) were detected throughout the course of this experiment. During all time periods when cyclotron ion-source maintenance was required, during the two day weekend period when the experiment was interrupted, and after the experiment was completed, background spectra were accumulated because substantial corrections for the presence of long-lived spontaneous-fission activities were necessary. Fission decay with a $(2.6 \pm 0.5)$-h half-life was observed in these background measurements and we have ascribed most of the background fission events to the nuclide $^{256}$Fm ($t_{1/2} = 2.62 \pm 0.22$ h). This nuclide would be produced continuously during the experiment both directly and via the electron-capture decay of 76-min $^{256}$Md. In addition, in the electron-capture decay of $^{256}$Md, sufficient energy is imparted to the recoil atom to transfer some $^{256}$Fm directly to the face of the surface-barrier detector. This transfer mechanism has been verified by us,[43] and as applied to this present experiment, the $^{256}$Fm spontaneous-fission background level in the main detector, as deduced from the number of events in the second surface-barrier detector, was underestimated by ~30%.

Sufficient "beam-off" background data were accumulated to assess the level of singles fission events arising from all relatively long-lived background sources which interefered with our ex-

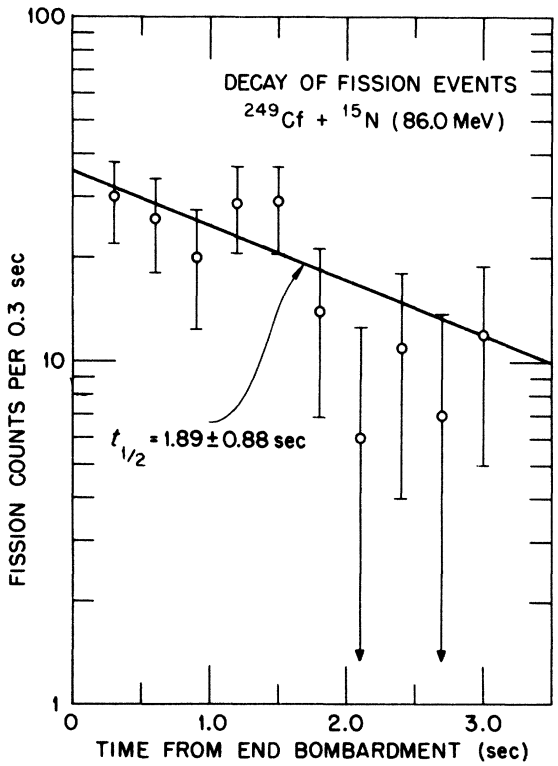


FIG. 5. Time distribution of single-fragment spontaneous-fission events following bombardment of $^{249}$Cf with 86.0-MeV $^{15}$N ions. A background subtraction of 20 events per 0.3-sec interval has been performed.

periments with $^{260}105$. Over 50% of the 388 single-fragment fission events observed are due to long-lived background sources, and the time distribution of the events remaining after background subtraction is shown in Fig. 5. These remaining 184 events decayed with a half-life of $1.89 \pm 0.88$ sec as derived from a one-component least-squares fitting procedure. The uncertainties for the number of events in each 0.3-sec time bin in Fig. 5 also include those of the background level.

Although it is exceedingly difficult to attribute spontaneous-fission events to the decay of a particular nuclide because of the nonspecificity of the decay process, the agreement of the half life derived above, $1.89 \pm 0.88$ sec, with the half-life observed for the $\alpha$ decay of $^{260}105$, $1.52 \pm 0.13$ sec, suggests that the fission events could in fact be associated with the decay of $^{260}105$. If all of the fission events that decay with a $1.89 \pm 0.88$-sec half-life, $184 \pm 24$ total in Fig. 5, are associated with the decay of $^{260}105$, the resultant spontaneous-fission decay branch would be $(9.6 \pm 0.6)\%$. This apparent fission-decay branch result is in agreement with the upper limit of 20% placed on this decay mode by Ghiorso *et al.*[8]) No readily apparent preference for symmetric fission was observed from our single-fragment kinetic-energy distribution, and, in fact, a thorough analysis of the mass and energy distributions from coincident double-fragment measurements would be required to confirm this effect.

### C. Coincident photon measurements

#### *1. Post α-decay photon spectra*

As described in Sec. IIC, events occurring in the photon detector during the ~80-$\mu$sec TPHA conversion interval following an $\alpha$ event were digitized and recorded together with the corresponding $\alpha$ event and the THPA signal. Photons in either prompt or delayed coincidence with particular $\alpha$-energy groups were extracted from scans of the list-mode data. The various $L$- and $K$-series x rays of Cm and the $\gamma$ rays which arise in the $\alpha$ decay of $^{249}$Cf provided convenient internal photon coincidence standards as $^{249}$Cf recoils resulting from inelastic and elastic scattering were among the reaction products.

The photon spectrum in the energy range 10–35 keV in prompt coincidence ($2\tau \leq 200$ nsec) with $\alpha$ particles in the energy range 9.00–9.20 MeV (i.e., those expected in the decay of $^{260}105$) is shown in Fig. 6. The $L$-series x rays of the heaviest elements occur in this photon energy range, and because nearly all of the statistically significant coincidence events associated with the 9.00–9.20 MeV $\alpha$ groups are contained in the spectrum of

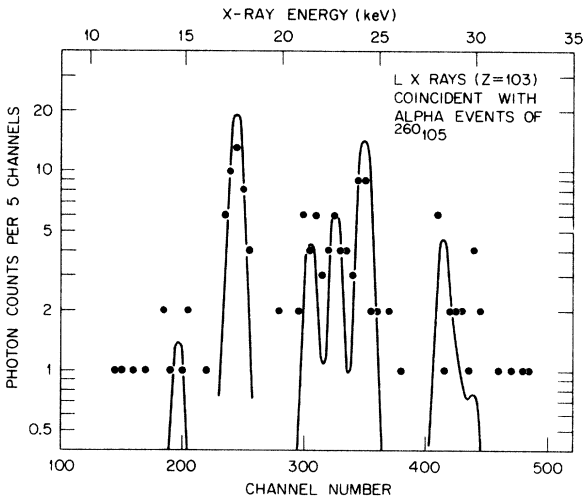


FIG. 6. Prompt coincidence photon spectrum in the energy range 10–35 keV associated with $\alpha$ events in the energy range 9.00–9.20 MeV.

Fig. 6, we have used these $L$ x rays to support our elemental assignment of $Z = 105$. The recent recommendations for the electron binding energies of Lr ($Z = 103$) of Porter and Freedman,[38] which are based on modest extrapolations of experimental data evaluated thru Fm ($Z = 100$), were used to predict the theoretical $L$ x-ray energies; the calculated radiative transition rates of Scofield[44] were used to predict the relative intensities. These calculated energies and relative intensities for the most prominent $L$-series x rays of Lr ($Z = 103$) are listed in Table I. It should be noted that binding energy calculations ($95 \leq Z \leq 130$) have also been performed by Carlson and Nestor,[45] and the agreement at $Z = 103$ with the highest $Z$ entry in the evaluations of Porter and Freedman[38] is excellent.

A spectrum was constructed for each $L$ subshell for Lr using the energies and relative intensities in Table I folded with the instrumental response of the Ge detector. These spectra were then normalized in amplitude to the most intense lines, the $L\alpha_1 + L\alpha_2$, $L\beta_1$, and $L\beta_4$ lines in the spectrum shown in Fig. 6. The solid curve in Fig. 6 is the composite calculated spectrum, and the agreement with the experimental data is quite apparent despite the poor statistical accuracy. The spectra expected for other elements, particularly to the adjacent No ($Z = 102$) and $Z = 104$ elements, could not be fitted to the spectrum in Fig. 6. The changes in energy for a one unit change in atomic number at $Z = 103$ are in the range 600–800 eV for the most intense transitions arising from $L_{\mathrm{I}}$- and $L_{\mathrm{II}}$-subshell vacancies, and in the range 250–500 eV for those transitions arising from $L_{\mathrm{III}}$-subshell vacancies, which are very substantial shifts

TABLE I. Energies in keV and relative intensities for the prominent $L$-series x rays of Lr ($Z = 103$).

| Shell | Line | Theoretical energy[a] | Theoretical Relative intensity[b] | Experimental energy |
|---|---|---|---|---|
| $L_{\mathrm{I}}$ | $L\beta_4(M_{\mathrm{II}})$ | 22.619 ± 0.015 | 1.000[c] | 22.61 ± 0.18 |
| | $L\beta_3(M_{\mathrm{III}})$ | 24.223 ± 0.015 | 0.601 | ••• |
| | $L\beta_{10}(M_{\mathrm{IV}})$ | 24.907 ± 0.018 | 0.059 | ••• |
| | $L\beta_9(M_{\mathrm{V}})$ | 25.207 ± 0.019 | 0.087 | ••• |
| | $L\gamma_2(N_{\mathrm{II}})$ | 28.120 ± 0.023 | 0.289 | ••• |
| | $L\gamma_3(N_{\mathrm{III}})$ | 28.560 ± 0.021 | 0.208 | ••• |
| | $L\gamma_4(O_{\mathrm{II-III}})$ | 29.654 ± 0.023 ($O_{\mathrm{II}}$) | 0.133 | ••• |
| $L_{\mathrm{II}}$ | $L\beta_1(M_{\mathrm{IV}})$ | 23.927 ± 0.018 | 1.000[c] | 24.03 ± 0.14 |
| | $L\gamma_1(N_{\mathrm{IV}})$ | 27.911 ± 0.022 | 0.249 | 27.97 ± 0.15 |
| | $L\gamma_6(O_{\mathrm{IV}})$ | 28.929 ± 0.017 | 0.056 | ••• |
| $L_{\mathrm{III}}$ | $Ll(M_{\mathrm{I}})$ | 14.429 ± 0.016 | 0.083 | 14.43 ± 0.20 |
| | $L\alpha_2(M_{\mathrm{IV}})$ | 17.183 ± 0.016 | 0.114 | ••• |
| | $L\alpha_1(M_{\mathrm{V}})$ | 17.483 ± 0.018 | 1.000[c] | 17.57 ± 0.12 |
| | $L\beta_2(N_{\mathrm{V}})$ | 21.247 ± 0.026 | 0.225 | 21.35 ± 0.20 |
| | $L\beta_5(O_{\mathrm{IV-V}})$ | 22.185 ± 0.016 ($O_{\mathrm{IV}}$) | 0.054 | ••• |

[a]Adapted from Porter and Freedman, Ref. 38.

[b]Adapted from Scofield, Ref. 44.

[c]Radiative transitions arising from the same $L$ vacancy were normalized to the strongest transition.

when compared to the detector resolution width of ~280 eV full width at half maximum (FWHM). Because the correspondence in energy and intensity predicted for $L$-series x rays with those of the most intense lines in Fig. 6, the $L$ x-ray "fingerprint," is unique for element 103 (Lr), and because these transitions were observed in coincidence with $\alpha$ particles, the atomic number of the $\alpha$-emitting parent nuclide is unambiguously established as $Z = 105$. Elemental identifications based on $L$ x rays for the heaviest elements as above are not as straightforward as those based on the observations of $K$ x rays performed previously for No[2] and for element 104.[3] A larger number of events is required to identify the $L$ x-ray "fingerprint," at least the $L\alpha_{1+2}$, $L\beta_2$, $L\beta_1$, and $L\gamma_1$ lines. The spectrum shown in Fig. 6 contains 151 total $L$ x rays, which is at least the minimum number required to perform such an identification in the absence of background events; this spectrum contains more than 10 times the number of x rays than were required for a similar identification of element 104 based on the use of $K$-series x rays.[3]

All $\alpha$ groups in the range 9.00–9.20 MeV produced $L$ x rays of Lr, indicating that none of these groups correspond to the transition from $^{260}$105 to the ground state of $^{256}$Lr. A few photon events (15 total) in prompt coincidence with these $\alpha$ particles occur in two distinct groups at energies of 41.1 ± 0.2 and 48.8 ± 0.3 keV which we attribute to true coincidence $L$ x-ray–$L$ x-ray sum events which arise from internally converted cascade nuclear transitions in $^{256}$Lr. No other two or more photon events in the range 50–450 keV with an energy spacing of $\lesssim$500 eV were detected in prompt coincidence with 9.00–9.20 MeV $\alpha$ particles. We are thus able to place an upper limit of 1.5% per decay on the yield of low-energy $\gamma$ rays and $K$-series x rays of Lr in the decay of $^{260}$105. The absence of the $K$-series x rays, within the above intensity limit, also allows an upper energy limit of 153 keV, the $K$-shell binding energy of Lr, to be placed on any nuclear transition, internally converted or not, in $^{256}$Lr. The yield of $L$ x rays of Lr in the decay of $^{260}$105 is (69 ± 7)% per decay, which implies that every $\alpha$ transition of $^{260}$105 results in one or more $L$-subshell vacancies as based on estimates[46,47] of the rates of radiative, Auger, and Coster-Kronig processes for the $L$ subshells of Lr.

### 2. *Search for x rays preceding fission*

A special feature of the data acquisition system allowed photons in the $L$- and $K$-series energy bands for the elements $Z = 99$–105 occurring in time prior to the occurrence of fission events to be recorded, and the event times to be established to an accuracy of ±10 nsec. If the nuclide $^{260}$105 decayed via electron capture to $^{260}$104, which then in turn spontaneously fissioned, the fission events would have been recorded in delayed coincidence

with x rays characteristic of element 104 in our experiments. As described in the previous section, 388 single-fragment-fission events were recorded in the course of this experiment, 184 ± 24 of which decayed with a half-life consistent with that observed for the $\alpha$ decay of $^{260}$105. These fissions could have arisen from the spontaneous fission of $^{260}$104, via the decay of $^{260}$105, if the half-life of $^{260}$104 were substantially shorter than that of $^{260}$105. From an experimental viewpoint, the influence of random coincidence correlations becomes a severe limitation of the approach outlined above if the half-life of $^{260}$104 is longer than a few msec as the average singles photon counting rate in the acceptable $L$ and $K$ x-ray energy bands was 1000–2000 counts per second throughout this experiment. Most of these photons were radiations from short-lived fission products by the $^{15}$N-ion fission of the $^{249}$Cf target.

We have diligently examined the ~50 magnetic tapes containing the prior x-ray data without finding any statistically significant correlations between the x rays characteristic of element 104 followed by fission events. From the complete absence of x rays characteristic of element 104 in a time interval of 110 $\mu$sec prior to the occurrence of any of the 388 total fission events observed in these experiments, we are able to place an upper limit of 0.2% on the electron-capture decay branching of $^{260}$105 if the half-life of $^{260}$104 is $\lesssim$100 $\mu$sec. If the latest revised half-life value[28] of 80 ± 20 msec suggested for $^{260}$104 is used, our experiments are severely affected by random coincidence correlations, and we are able to place an upper limit only of 2.5% at the 90% confidence level on the electron-capture branching decay of $^{260}$105.

In our attempts to extract delayed coincidence 104 x-ray–fission correlations from these data, suggestions of statistically significant correlations between the $K\alpha_2$ and $K\alpha_1$ x rays expected for element 103 at energies of 123.92 and 130.66 keV, followed by fission in a time interval $\leq$40 msec, continually recurred. We were unsuccessful in establishing these correlations firmly by restricting the digital ranges of the various parameters which would characterize events of this type because of the influence of random coincidence correlations. From an analysis of the time distribution of these events, a half-life of 21 ± 16 msec could be derived. We mention this result, despite our inability to establish this correlation firmly from statistical considerations, only because of the recent report[30] of the production of a 20.1 ± 1.7 msec spontaneous-fission activity in $^{15}$N-ion bombardments of $^{249}$Bk. The identity of this 20-msec fission activity is unknown, but if the interpretation of our results is correct, the 20-msec activity could be an isotope of Lr which most certainly could have been produced in the $^{249}$Bk + $^{15}$N reaction of Ghiorso.[30]

## IV. CONCLUSIONS

A summary of the $\alpha$-particle energy and intensity results for (1.52 ± 0.13)-sec $^{260}$105 is given in Table II. The spontaneous-fission events decaying with the (1.89 ± 0.88)-sec half-life have been ascribed to the direct spontaneous-fission branching decay of $^{260}$105. This spontaneous-fission branching accounts for (9.6 ± 0.6)% of the decays of $^{260}$105 and an upper limit of 2.5% has been placed on the electron-capture decay to $^{260}$104, if $^{260}$104 is an 80 ± 20 msec spontaneous-fission activity. If the nuclide $^{260}$104 has a half-life of <110 $\mu$sec, the electron-capture branching decay of $^{260}$105 is $\leq$0.2%.

$\alpha$-decay hindrance factors for these groups have been calculated using the spin-independent ($l = 0$) equations of Preston.[48] We have used an adjusted radius parameter $r_0$ of 1.468 fm in this calculation; the resultant hindrance factors are listed in Table II. Because $L$-series x rays of Lr were observed in coincidence with all three of the $\alpha$ groups listed in Table II, we are unable to establish the total $\alpha$-decay energy $Q_\alpha$ for $^{260}$105. However, the highest energy $\alpha$ group, the 9.120 MeV group, implies a $Q_\alpha$ value of at least 9.306 ± 0.017 MeV, and if an additional 22.4 keV, the $L_{III}$ binding energy for Lr, is included to account for our coincident x-ray observations, the minimum $Q_\alpha$ value if 9.328 ± 0.017 MeV.

The assignments of these $\alpha$ groups to the decay of $^{260}$105 have been verified by the establishment of a direct genetic linkage to the $\alpha$-decay daughter nuclide $^{256}$Lr. The elemental assignment of $Z = 105$ has also been established by the observation of $L$ x rays of Lr in coincidence with these $\alpha$ groups. No $\gamma$ rays were observed in coincidence so that it is not possible to establish nuclear energy levels in $^{256}$Lr.

On the basis of our experimental information on the decay of $^{260}$105, we may summarize our conclusions as follows: (1) We have produced in the

TABLE II. Summary of $\alpha$-particle energy and intensity results for $^{260}$105; total $\alpha$ decay is 90.4 ± 0.6%; spontaneous fission is 9.6 ± 0.6%.

| $\alpha$-particle energy (MeV) | Intensity (% decay) | Hindrance factor |
|---|---|---|
| 9.041 ± 0.014 | 48 ± 5 | 5.8 ± 0.6 |
| 9.074 ± 0.014 | 25 ± 3 | 13 ± 2 |
| 9.120 ± 0.017 | 17 ± 3 | 28 ± 5 |

reaction of $^{15}N$ with $^{249}Cf$ a 1.52-sec $\alpha$ activity with $\alpha$-particle groups at 9.04, 9.07, 9.12 MeV, similar to the results of the earlier experiments of Ghiorso *et al.*[8] (2) In addition, we have definitively established the atomic number for this activity as 105 and established the mass number as 260. (3) We see no evidence of the 8.9-, 9.4-, or 9.7-MeV $\alpha$-particle groups in the decay of $^{260}105$ as reported in Ref. 12 and Ref. 17. (4) We do detect a spontaneous-fission activity with a half-life similar to that for $^{260}105$ derived from $\alpha$-decay data, but beyond this similarity we are unable to establish a definitive link between these activities.

Our results for $^{260}105$ completely corroborate and extend the earlier experiments of Ghiorso *et al.*[8] The unique identification provided for element 105 in our present experiments unequivocally supports the discovery claims for element 105 proffered by Ghiorso *et al.*[8]

## ACKNOWLEDGMENTS

We wish to thank the ORIC operations crew, E. D. Hudson and Dr. M. L. Mallory, for invaluable assistance in providing the intense $^{15}N$ ion beam used in these experiments. Assistance from the staff of the Transuranium Research Laboratory is gratefully acknowledged.

---

†Research sponsored by the Division of Physical Research of the U.S. Energy Research and Development Administration under contract with Union Carbide Corporation.

[1]C. E. Bemis, Jr., in *Proceedings of International Conference on Reactions Between Complex Nuclei, Nashville, Tennessee, 1974,* edited by R. L. Robinson, F. K. McGowan, J. B. Ball, and J. H. Hamilton (North-Holland, Amsterdam/American-Elsevier, New York, 1974), Vol. II, p. 529.

[2]P. F. Dittner, C. E. Bemis, Jr., D. C. Hensley, R. J. Silva, and C. D. Goodman, Phys. Rev. Lett. 26, 1037 (1971).

[3]C. E. Bemis, Jr., R. J. Silva, D. C. Hensley, O. L. Keller, Jr., J. R. Tarrant, L. D. Hunt, P. F. Dittner, R. L. Hahn, and C. D. Goodman, Phys. Rev. Lett. 31, 647 (1973).

[4]C. E. Bemis, Jr., P. F. Dittner, D. C. Hensley, C. D. Goodman, and R. J. Silva, Oak Ridge National Laboratory Report No. ORNL-4706, September 1971 (unpublished), p. 62.

[5]C. E. Bemis, Jr., P. F. Dittner, C. D. Goodman, D. C. Hensley, K. Kumar, and R. J. Silva, Oak Ridge National Laboratory Report No. ORNL-4706, (unpublished), p. 64.

[6]C. E. Bemis, Jr., R. J. Silva, D. C. Hensley, O. L. Keller, Jr., J. R. Tarrant, L. D. Hunt, P. F. Dittner, R. L. Hahn and C. D. Goodman, Oak Ridge National Laboratory Report No. ORNL-4976, October 1974, (unpublished), p. 37.

[7]A. Ghiorso, M. Nurmia, J. Harris, K. Eskola, and P. Eskola, Phys. Rev. Lett. 22, 1317 (1969).

[8]A. Ghiorso, M. Nurmia, K. Eskola, J. Harris, and P. Eskola, Phys. Rev. Lett. 24, 1498 (1970).

[9]A. Ghiorso, M. Nurmia, K. Eskola, and P. Eskola, Phys. Rev. C 4, 1850 (1971).

[10]A. Ghiorso, M. Nitschke, J. R. Alonso, M. Nurmia, G. T. Seaborg, E. K. Hulet, and R. W. Lougheed, Phys. Rev. Lett. 33, 1490 (1974).

[11]G. N. Flerov, J. Phys. Soc. Jpn. (Suppl.) 24, 237 (1968).

[12]G. N. Flerov, V. A. Druin, A. G. Demin, Yu. V. Lobanov, N. K. Skobelev, G. N. Akapiev, B. V. Fefilov, I. V. Kolesov, K. A. Gavrilov, Yu. P. Kharitonov, and L. P. Chelnokov, Joint Institute for Nuclear Research Report No. JINR P7-3808, Dubna, USSR, 1968 (unpublished).

[13]G. N. Flerov, Yu. Ts. Oganesyan, Yu. V. Lobanov, Yu. A. Lazarev, and S. P. Tretiakova, Joint Institute for Nuclear Research Report No. JINR P7-4932, Dubna, USSR, 1970 (unpublished).

[14]G. N. Flerov, Yu. Ts. Oganesyan, Yu. V. Lobanov, Yu. A. Lazarev, V. I. Kuznetsov, and S. P. Tretiakova, Joint Institute for Nuclear Research Report No. JINR P7-5108, Dubna, USSR, 1970 (unpublished).

[15]G. N. Flerov, Yu. Ts. Oganesyan, Yu. V. Lobanov, Yu. A. Lazarev, S. P. Tretiakova, I. V. Kolesov, and V. M. Plotko, At. Energ. 29, 243 (1970) [Sov. J. At. Energy 29, 967 (1971)]; Nucl. Phys. A160, 181 (1971).

[16]I. Zvara, V. Z. Belov, Yu. S. Korotkin, M. R. Shalayevsky, V. A. Shchegolev, M. Hussonnois, and B. A. Zager, Joint Institute for Nuclear Research Report No. JINR P12-5120, Dubna, USSR, 1970 (unpublished).

[17]V. A. Druin, A. G. Demin, Yu. P. Khartonov, G. N. Akapiev, V. I. Rud., G. Ya. Sun-Tzin-Yan, L. P. Chelnokov, and K. V. Gavrilov, Yad. Fiz. 13, 251 (1971) [Sov. J. Nucl. Phys. 13, 139 (1971)].

[18]G. N. Flerov, Yu. A. Lazarev, Yu. V. Lobanov, Yu. Ts. Oganesyan, and S. P. Tretiakova, in Proceedings of International Conference on Heavy Ion Physics, [Joint Institute for Nuclear Research Report No D7-5769, Dubna, USSR 1971 (unpublished)], p. 125; [translation: Oak Ridge National Laboratory Report No. ORNL-tr-2711 (unpublished)].

[19]I. Zvara, V. Z. Belov, V. P. Domanov, and M. R. Shalayevsky, Radiokymiya, 18, 371 (1976) [Sov. Radiochem. 18, 328 (1976)].

[20]G. N. Flerov, Yu. Ts. Oganesyan, Yu. V. Lobanov, V. I. Kuznetsov, V. A. Druin, V. P. Perelygin, K. A. Gavrilov, S. P. Tretiakova, and V. M. Plotko, At. Energ. 17, 310 (1964) [Sov. J. At. Energy 17, 1046 (1964)].

[21]Yu. Ts. Oganesyan, Yu. V. Lobanov, S. P. Tretiakova, Yu. A. Lazarev, I. V. Kolesov, K. A. Gavrilov, V. M. Plotko, and Yu. V. Polubarinov, At. Energ. 28, 393 (1970) [Sov. J. At. Energy 28, 502 (1970)].

[22]A. Ghiorso, M. Nurmia, and J. Harris, Univ. of California Lawrence Radiation Laboratory Report No. UCRL-18714, Berkeley, California, 1969 (unpublished).

[23]V. A. Druin, in *Nuclear Reactions Induced by Heavy Ions,* edited by R. Boch and W. R. Herring (North-Holland, Amsterdam, 1970), p. 657.

[24]M. Nurmia (see Ref. 23), p. 666.
[25]A. Ghiorso, in *Proceedings of the Robert A. Welch Foundation Conference on Chemical Research XIII, The Transuranium Elements——The Mendeleev Centennial,* edited by W. O. Milligan (Welch Foundation, Houston, Texas, 1970), p. 107.
[26]I. Zvara (see Ref. 25), p. 153.
[27]M. Nurmia, E. K. Hulet, K. Williams, and A. Ghiorso, Lawrence Berkeley Laboratory Report No. LBL-4000, Berkeley, California, (unpublished), p. 50.
[28]V. A. Druin, Yu. S. Korotkin, Yu. V. Lobanov, Yu. V. Poluboyarinov, R. N. Sagaidak, G. M. Solovyova, S. P. Tretyakova, and Yu. P. Kharitonov, Yad. Fiz. 24, 254 (1976) [Sov. J. Nucl. Phys. 24, 131 (1976)].
[29]G. N. Flerov, in *Proceedings of the Third International Conference on Nuclei Far From Stability, Cargèse, Corsica, France May 1976* (CERN 76-13, Geneva, 1976), p. 542.
[30]A. Ghiorso (see Ref. 29), p. 548.
[31]C. E. Bemis, Jr., R. L. Ferguson, F. Plasil, R. J. Silva, F. Pleasonton, and R. L. Hahn, Phys. Rev. C 15, 705 (1977).
[32]T. Sikkeland, A. Ghiorso, and M. Nurmia, Phys. Rev. 172, 1232 (1968).
[33]T. Sikkeland, J. Maly, and D. F. Lebeck, Phys. Rev. 169, 1000 (1968).
[34]A. S. Iljinov, Joint Institute for Nuclear Research Report, JINR P7-7108, Dubna, USSR, 1973 [translation Oak Ridge National Laboratory Report No. ORNL-tr-2701, Oak Ridge, Tennessee, 1973 (unpublished)].
[35]C. D. Goodman, C. A. Ludemann, D. C. Hensley, R. Kurz, and E. W. Anderson, IEEE Trans. Nucl. Sci. NS-18, (1), 323 (1971); C. D. Goodman, Oak Ridge National Laboratory Report No. ORNL-TM-3946, 1972 (unpublished).
[36]D. C. Hensley, IEEE Trans. Nucl. Sci. 20, 334 (1973).
[37]A. Rytz, At. Data Nucl. Data Tables 12, 479 (1973).
[38]F. T. Porter and M. S. Freedman, Recommended Atomic Electron Binding Energies for the Heavy Elements, $Z = 84$ to 103 (to be published).
[39]C. E. Bemis, Jr., R. E. Goans, W. M. Good, and G. G. Warner, in *Proceedings of the Ninth Midyear Topical Symposium of Health Physics Society* (University of Denver, Denver, 1976), p. 578.
[40]I. Ahmad and M. Waldgren, Nucl. Instrum. Methods 99, 333 (1972).
[41]K. Eskola, P. Eskola, M. Nurmia, and A. Ghiorso, Phys. Rev. C 4, 632 (1971).
[42]C. E. Bemis, Jr., P. F. Dittner, R. J. Silva, D. C. Hensley, R. L. Hahn, J. R. Tarrant, and L. D. Hunt, Oak Ridge National Laboratory Report No. ORNL-5111, Oak Ridge, Tenn., 1976 (unpublished), p. 58.
[43]C. E. Bemis, Jr., R. L. Ferguson, R. J. Silva, F. Plasil, G. D. O'Kelley, R. L. Hahn, D. C. Hensley, E. K. Hulet, and R. W. Lougheed, Bull. Am. Phys. Soc. 22, 611 (1977); and (unpublished).
[44]J. H. Scofield, At. Data Nucl. Data Tables 14, 121 (1974).
[45]T. A. Carlson and C. W. Nestor, Jr., At. Data Nucl. Data Tables 19, 153 (1977).
[46]O. Keski-Rahkonen and M. O. Krause, At. Data Nucl. Data Tables 14, 139 (1974).
[47]M. O. Krause (private communication).
[48]M. A. Preston, Phys. Rev. 71, 865 (1947).

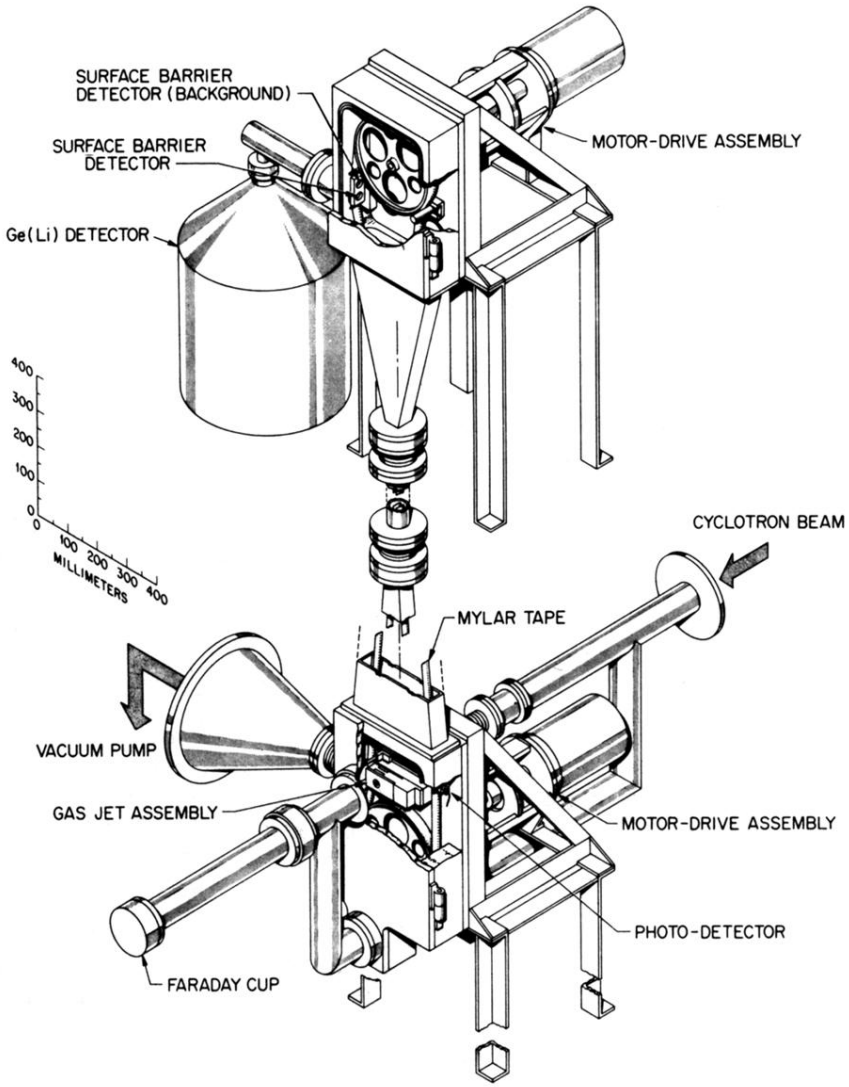


FIG. 1. Cutaway view of the tape-transport system and gas-jet assembly used to transfer reaction product recoil atoms to the detection station.